

# Measurement of Fast Dimerization Rates by Cyclic Voltammetry: Comparison of the 17e Radicals ( $\eta^5\text{-C}_5\text{R}_5$ )Cr(CO)<sub>3</sub> (R = H, CH<sub>3</sub>) at Low Temperatures

Thomas C. Richards and William E. Geiger\*

Department of Chemistry, University of Vermont, Burlington, Vermont 05405

Michael C. Baird

Department of Chemistry, Queen's University, Kingston, Ontario, Canada K7L 3N6

Received June 16, 1994<sup>®</sup>

The 17e complexes ( $\eta^5\text{-C}_5\text{H}_5$ )Cr(CO)<sub>3</sub> (**2**) and ( $\eta^5\text{-C}_5\text{Me}_5$ )Cr(CO)<sub>3</sub> (**3**) are in equilibrium with their metal–metal-bonded dimers **2**<sub>2</sub> and **3**<sub>2</sub>, respectively. Cyclic voltammetry (CV) studies of the two complexes reveal details of both the equilibrium concentrations of monomers and dimers (at high CV sweep rates) and the rates of interconversion between the monomers and dimers (at lower sweep rates). Voltammetry was performed in CH<sub>2</sub>Cl<sub>2</sub>/0.1 M [Bu<sub>4</sub>N][PF<sub>6</sub>] electrolyte. At room temperature and slow to moderate scan rates, a single Nernstian wave is seen for both complexes, arising from reduction of the monomer by one electron,  $E^\circ = -0.82$  V vs Fc for **2/2**<sup>-</sup> and  $-0.93$  V for **3/3**<sup>-</sup>. High sweep rates (up to several thousand volts per second) are required to freeze out the monomer/dimer rates at  $T < 250$  K. Digital simulations of CV curves corrected for background currents and ohmic effects establish a dimerization rate constant for **2** in this medium at 243 K of  $8.4 \times 10^5$  M<sup>-1</sup> s<sup>-1</sup>, whereas a larger value is found for the permethylated analogue **3** at 228 K,  $1.7 \times 10^7$  M<sup>-1</sup> s<sup>-1</sup>. These values are compared to those previously reported in laser flash photolysis studies at room temperature.

## Introduction

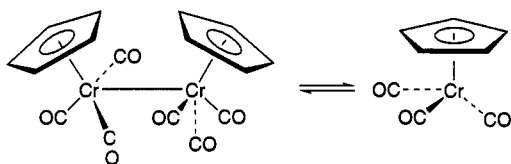
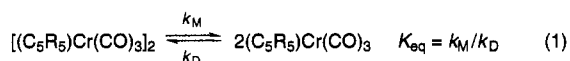
The family of 17-electron (17e) radicals ( $\eta^5\text{-C}_5\text{R}_5$ )M(CO)<sub>3</sub> (**1**; M = Cr, Mo, W) has come under intense scrutiny with respect to its chemical and physical properties.<sup>1</sup> This interest derives in part from recognition of the importance of organometallic radicals as intermediates and in part from the synthetic accessibility and robustness of this system.<sup>2,3</sup> Solutions of **1** are in equilibrium with the corresponding metal–metal-bonded dimer (eq 1).<sup>1–4</sup> Detectable equilibrium quanti-

ties of radicals are observed only for the M = Cr system, implying that  $K_{\text{eq}} \ll 1$  for the Mo and W complexes.<sup>4</sup> Equilibrium constants for the Cr complexes with R = H, Me, as measured or estimated by ESR,<sup>5,6</sup> NMR,<sup>1a,7</sup>

IR,<sup>1a,8</sup> and UV–vis,<sup>8</sup> have been recently summarized and discussed.<sup>1a</sup> By way of contrast, there have been few reports concerning the kinetics of these systems,<sup>9,10</sup> so that serious ambiguities remain concerning the mechanism of reactions involving these radicals, especially regarding the importance of the 17e/19e equilibrium of eq 2 and the role of radical disproportionation processes.<sup>1c,5,11,12</sup>



Voltammetry is well equipped to answer some of these questions, and although a number of electrochemical studies of these systems have appeared,<sup>12,13</sup> no dimerization rate constants have been published based on these data. Since knowledge of  $k_M$  and  $k_D$  is of obvious import in a quantitative treatment of the rates and mechanisms of the reactions of **1**, we now report such



ties of radicals are observed only for the M = Cr system, implying that  $K_{\text{eq}} \ll 1$  for the Mo and W complexes.<sup>4</sup> Equilibrium constants for the Cr complexes with R = H, Me, as measured or estimated by ESR,<sup>5,6</sup> NMR,<sup>1a,7</sup>

<sup>®</sup> Abstract published in *Advance ACS Abstracts*, October 1, 1994.

(1) (a) Watkins, W. C.; Jaeger, T.; Kidd, C. E.; Fortier, S.; Baird, M. C.; Kiss, G.; Roper, G. C.; Hoff, C. D. *J. Am. Chem. Soc.* **1992**, *114*, 907. (b) Scott, S. L.; Espenson, J. H.; Zhu, Z. *J. Am. Chem. Soc.* **1993**, *115*, 1789. (c) Brown, T. L. In *Organometallic Radical Processes*; Trogler, W. C., Ed.; Elsevier: Amsterdam, 1990; p 67 ff. See also references contained in ref 1a–c.

(2) Adams, R. D.; Collins, D. E.; Cotton, F. A. *J. Am. Chem. Soc.* **1974**, *96*, 749.

(3) (a) Jaeger, T. J.; Baird, M. C. *Organometallics* **1988**, *7*, 2074. (b) Goh, L. Y.; Hambley, T. W.; Darenbourg, D. J.; Reibenspies, J. J. *Organomet. Chem.* **1990**, *381*, 349.

(4) Drake, P. R.; Baird, M. C. *J. Organomet. Chem.* **1989**, *363*, 131.

(5) Madach, T.; Vahrenkamp, H. *Z. Naturforsch., B* **1978**, *33B*, 1301.

(6) Fortier, S.; Baird, M. C.; Preston, K. F.; Morton, J. R.; Ziegler, T.; Jaeger, T.; Watkins, W. C.; MacNeil, J. H.; Watson, K. A.; Hensel, K.; Le Page, Y.; Charland, J. P.; Williams, A. *J. Am. Chem. Soc.* **1991**, *113*, 542.

(7) Goh, L. Y.; Khoo, S. K.; Lim, Y. Y. *J. Organomet. Chem.* **1990**, *399*, 115.

(8) McLain, S. J. *J. Am. Chem. Soc.* **1988**, *110*, 643.

(9) (a) Meyer, T. J.; Caspar, J. V. *Chem. Rev.* **1985**, *85*, 187. (b) Hughey, J. L.; Bock, C. R.; Meyer, T. J. *J. Am. Chem. Soc.* **1975**, *97*, 4440. (c) van Vlierberge, B. A.; Abrahamson, H. B. *J. Photochem. Photobiol. A* **1990**, *52*, 69.

(10) Yao, Q.; Bakac, A.; Espenson, J. H. *Organometallics* **1993**, *12*, 2010.

(11) (a) Hepp, A. F.; Wrighton, M. S. *J. Am. Chem. Soc.* **1981**, *103*, 1258. (b) Scott, S. L.; Espenson, J. H.; Chen, W.-J. *Organometallics* **1993**, *12*, 4077. (c) Blaha, J. P.; Wrighton, M. S. *J. Am. Chem. Soc.* **1985**, *107*, 2694. (d) Tyler, D. R.; Philbin, C.; Fei, M. In *Paramagnetic Organometallic Species in Activation/Selectivity, Catalysis*; Chanon, M.; Julliard, M.; Poite, J. C., Eds.; Kluwer: Dordrecht, The Netherlands, 1989; p 209.

(12) Tilstet, M. *Inorg. Chem.* **1994**, *33*, 3121.

rate constants from low-temperature cyclic voltammetry (CV) data on  $\text{CpCr}(\text{CO})_3$  (**2**;  $\text{Cp} = \eta^5\text{-C}_5\text{H}_5$ ), and  $\text{Cp}^*\text{Cr}(\text{CO})_3$  (**3**;  $\text{Cp}^* = \eta^5\text{-C}_5\text{Me}_5$ ). After completion of our experiments,<sup>14</sup> a photochemical study yielding  $k_M$  and  $k_D$  for both **2** and **3** at room temperature was published.<sup>10</sup> Significantly different conclusions are made from the electrochemically vs photochemically derived sets of rate constants.

When one begins with an equilibrated mixture of monomer and dimer, measurement of dimerization rates by either electrochemistry or photochemistry relies on perturbation of the monomer concentration by electrodic or photolytic means, respectively. An advantage of CV for the study of reactive radicals is that the presence of side reactions, a significant concern for **2** and **3**,<sup>9b,10,15,16</sup> is readily diagnosed by the appearance of new voltammetric waves or decreased currents for analyte waves. Simulation of the CV curve over the pertinent potential regime provides the mass balance necessary to assure that kinetic conclusions are not being compromised by undiagnosed reactions coupled to the electron transfer.

A disadvantage of electrochemistry is that fast CV experiments require the presence of supporting electrolyte and reasonably polar solvents, which may affect the reaction mechanism if it is sensitive to the polarity of the medium or to ion-pairing effects. Since dichloromethane was used in order to minimize the possibility of solvent coordination to the 17e radical, analytical difficulties arose from the large ohmic loss associated with electrolyte solutions of  $\text{CH}_2\text{Cl}_2$  under conditions of low temperatures and high scan rates. Corrections for both background charging currents and ohmic loss were achieved, and experimental voltammograms were successfully modeled by digital simulations over a range of temperatures, scan rates, and concentrations.

CV scans of **2** or **3** display a single reversible wave at slow scan rates ( $v$ ) and ambient temperatures, as has been noted.<sup>5,13d,17</sup> At low temperatures, however, and/or short observation times (high  $v$ ) two cathodic waves are observed (vide infra). The relative contributions of these two waves, which arise separately from a monomer and its corresponding dimer, allow measurement of the relative concentrations of the two species during the voltammetric scan.

A surprising result was obtained: the dimerization rate of the pentamethylcyclopentadienyl complex **3** is faster than that of the cyclopentadienyl complex **2**, in spite of the former being more sterically encumbered. This conclusion is rationalized by invocation of a late transition state in the monomer to dimer conversion.

## Experimental Section

**General Considerations.** All operations were conducted under an atmosphere of  $\text{N}_2$  using dried and distilled solvents, following standard Schlenk procedures. Literature methods

(13) (a) Dessy, R. E.; Stary, F. E.; King, R. B.; Waldrop, M. *J. Am. Chem. Soc.* **1966**, *88*, 471. (b) Kadish, K. M.; Lacombe, D. A.; Anderson, J. E. *Inorg. Chem.* **1986**, *25*, 2246. (c) Pugh, J. R.; Meyer, T. J. *J. Am. Chem. Soc.* **1992**, *114*, 3784. (d) O'Callaghan, K. A. E.; Brown, S. J.; Page, J. A.; Baird, M. C.; Richards, T. C.; Geiger, W. E. *Organometallics* **1991**, *10*, 3119. (e) Tilset, M. *J. Am. Chem. Soc.* **1992**, *114*, 2740. (f) Tilset, M.; Parker, V. D. *J. Am. Chem. Soc.* **1989**, *111*, 6711.

(14) Richards, T. C. Ph.D. Dissertation, University of Vermont, 1992.

(15) Wrighton, M. S.; Ginley, D. S. *J. Am. Chem. Soc.* **1975**, *97*, 4246.

(16) Knorr, J. R.; Brown, T. L. *J. Am. Chem. Soc.* **1993**, *115*, 4087.

(17) Geiger, W. E. In *Progress in Inorganic Chemistry*; Lippard, S. J., Ed.; Wiley: New York, 1985; Vol. 33, pp 278-280.

were used to prepare  $[\text{CpCr}(\text{CO})_3]_2$  (**2a**) and  $[\text{Cp}^*\text{Cr}(\text{CO})_3]_2$  (**3a**): the former<sup>18</sup> at Queen's University, the latter<sup>6</sup> at the University of Vermont. Samples were stored under nitrogen at 248 K and recrystallized before use. Solutions of both radicals, but particularly those of the  $\text{Cp}^*$  complex, were highly air sensitive. Some decomposition of the radicals was noted after 1 h, even at 240 K in  $\text{CH}_2\text{Cl}_2$  in the drybox. Consequently, all scans reported in this work were acquired within 20 min of sample dissolution.

**Electrochemistry.** CV data were acquired with the electrochemical cell in a Vacuum Atmospheres drybox. Dichloromethane (reagent grade, various sources) was distilled from  $\text{CaH}_2$ , the last time in vacuo. The supporting electrolyte was  $[\text{Bu}_4\text{N}][\text{PF}_6]$ , prepared and dried as described.<sup>19</sup> The working electrodes were Pt disks of either commercial (1.4 mm diameter, Bioanalytical Systems) or homemade (495 and 125  $\mu\text{m}$  diameter) origin. The latter were made by sealing Pt wire (Goodfellow metals) through soft glass followed by treatment with an abrasive cloth. The smallest electrode was used only for CV scans in excess of 100 V/s. Polishing of the Pt disks included a final treatment with 0.25  $\mu\text{m}$  Metadi II diamond paste.

The reference electrode was a  $\text{Ag}/\text{AgCl}$  wire separated from the working electrode by at least 15 times the diameter of the latter, as necessary to employ resistance correction equations.<sup>20</sup> The potential of ferrocene (Fc)/ferrocenium was approximately +0.33 V against this reference. The potentials in this paper, however, are all reported vs Fc, which was added as an internal standard<sup>21</sup> at the end of each experiment. Data were collected on a Nicolet Model 4094C digital oscilloscope interfaced to a Princeton Applied Research Corporation Model 173/175 potentiostat/waveform system. Background scans were acquired under conditions identical with those of the sample scan for the purposes of eliminating charging currents and correcting voltammograms for resistance effects. The correction procedure utilized a computer program<sup>14</sup> that performed point-by-point resistance corrections and subtraction of background currents at each digitized potential. The cell temperature was controlled to a precision of  $\pm 0.1$  K by its immersion in a temperature-controlled heptane bath inside the drybox.

Resistivity values for solutions of  $\text{CH}_2\text{Cl}_2/0.1$  M  $[\text{Bu}_4\text{N}][\text{PF}_6]$  were obtained with a Beckman ac conductivity bridge, Model RC-18A, at a frequency of 1 kHz at Pt electrodes in a conductivity cell determined to have a cell constant of 0.326  $\text{cm}^{-1}$  at 297 K. Resistivities ranged from 743  $\Omega\text{ cm}$  at 298 K to 1529  $\Omega\text{ cm}$  at 223 K, and a full listing is available.<sup>14</sup>

The procedure for obtaining CV curves for comparison with simulations followed the recommendations of Bowyer *et al.*<sup>22</sup> The raw CV of the test compound was digitized and corrected for uncompensated resistance  $R_u$ , calculated from the relationship  $R_u = \rho/4r$ , where  $\rho$  is the resistivity ( $\Omega\text{ cm}$ ) and  $r$  is the electrode radius (cm). This equation holds for a disk separated from the reference electrode by at least several times  $r$ .<sup>20</sup> The background charging current was then subtracted from the resistance-corrected voltammogram to give a final trace against which to compare digital simulations. This procedure does not correct for the fact that the actual scan rate at the working electrode is altered by the changing magnitude of  $iR_u$  along the CV curve, where  $i$  is the current flowing at any potential. Since this effect can produce noticeable CV distortions in high-resistance solvents,<sup>22</sup> it was taken into account in the digital simulations, which adjusted the scan rate at each point in the calculated CV.

Digital simulations were performed utilizing the Fast Quasi-Explicit Finite Difference method<sup>23</sup> on either a VAX 8530

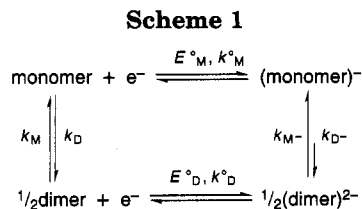
(18) Cooley, N. A.; MacConnachie, P. T. F.; Baird, M. C. *Polyhedron* **1988**, *7*, 1965.

(19) Pierce, D. T.; Geiger, W. E. *Inorg. Chem.* **1994**, *33*, 373.

(20) Newman, J. *J. Electrochem. Soc.* **1966**, *113*, 501.

(21) Gritzner, G.; Kuta, J. *Pure Appl. Chem.* **1984**, *56*, 461.

(22) Bowyer, W. J.; Engelman, E. E.; Evans, D. H. *J. Electroanal. Chem. Interfacial Electrochem.* **1989**, *262*, 67.



mainframe computer at UVM or on an IBM 3090 computer at the Cornell National Supercomputer Facility via Internet. In the simulations a diffusion coefficient ( $D_M$ ) of  $1 \times 10^{-5}$  cm<sup>2</sup>/s was assumed for both monomers (**2** and **3**), whereas  $D$  for the dimers was taken to be  $D_D = 6.8 \times 10^{-6}$  cm<sup>2</sup>/s, on the basis of the doubling of the molecular weight.<sup>24</sup> Changes in  $D$  had little effect on the simulations, except near or above the fast scan limit, where the peak current of the dimer wave is primarily affected. Values of  $D$  had, therefore, little effect on the primary object of the study, namely the dimerization rate constants.

## Results

**I. Qualitative Overview.** The mechanism of the reduction of the monomer/dimer mixture given in Scheme 1 is essentially that of a square scheme. Of the many possibilities arising from different combinations of formal potentials, rate constants, and equilibrium constants,<sup>25</sup> three limits are pertinent and help define the qualitative behavior of the system in CV experiments (in all cases it is assumed that  $E^\circ_M$ , the one-electron reduction potential of the monomer, is positive of  $E^\circ_D$ , the reduction potential of the dimer).

(a) The first is  $k_M/C^\circ \gg v$  (*slow scan limit*), in which  $k_M$  is the rate constant for "cracking" the neutral dimer into monomers (Scheme 1) and  $C^\circ$  is the formal concentration of the complex. This case results in a single response at the potential  $E^\circ_M$  even if the solution equilibrium favors the dimer. As the scan reaches a potential sufficient to reduce the monomer, perturbation of the equilibrium produces monomer faster than it can be reduced, giving a diffusion-controlled wave of full one-electron height. This condition is found under most experimental conditions for both **2** and **3**.

(b) The second is  $k_M/C^\circ \ll v$  (*fast scan limit*). In this case conversion from dimer to monomer is slow and the cathodic peak current associated with the monomer reduction is proportional to the equilibrium concentration of monomer. This condition, representing a "frozen" equilibrium, is reached for sub-millimolar concentrations of **2** at 240 K with scan rates above about 50 V/s and much higher scan rates for similar solutions of **3**.

(c) The third case is  $k_{M^-} \gg v$ . The reduction of the dimer is totally irreversible, giving 2 mol of the monomer monoanion, which is reoxidized to neutral monomer on the reverse sweep. Although we treated the dimer reduction as a quasi-reversible heterogeneous electron transfer (ET) process (rate constant  $k^0 = \text{ca } 10^{-3}$  cm/s) with a fast following monomerization reaction, this part of our treatment is not intended to be definitive. Various combinations of  $k^0$  and  $k_{M^-}$  would undoubtedly fit the observed traces for the second cathodic peak, as shown in an earlier related study of fulvalene com-

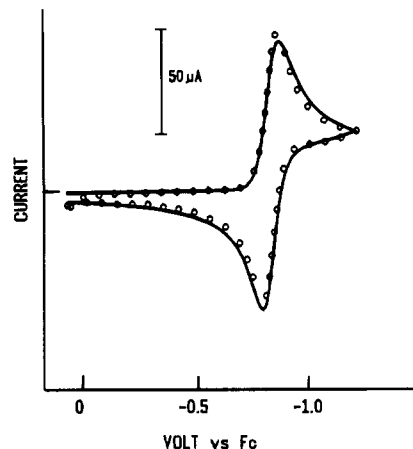
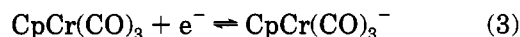


**Figure 1.** Comparison of experimental CV scan (circles) of a 0.9 mM solution of **2** in CH<sub>2</sub>Cl<sub>2</sub>/0.1 M [Bu<sub>4</sub>N][PF<sub>6</sub>] (293 K,  $v = 0.1$  V/s) at a 6.5 mm diameter Pt disk and theoretical simulation (solid line) of a Nernstian 1e couple with  $E^\circ = -0.82$  V vs Fc.

plexes.<sup>26</sup> Germane to the present study is that details of the irreversibility of the dimer reduction wave have little, if any, influence on the height or morphology of the first (monomer) wave and on the derived rate constants for neutral monomer/dimer equilibration.

**II. Study of CpCr(CO)<sub>3</sub>: Slow and Fast Scan Limits.** Figure 1 is a CV scan of formally 0.9 mM **2** at 293 K with  $v = 0.1$  V/s. The experimental curve has the characteristics of a diffusion-controlled Nernstian one-electron process, as shown by its close agreement with the theoretical values (circles) simulated on that basis. No features were noted at more negative potentials (in the dimer reduction regime), in spite of the fact that the dimer is the predominant species under these conditions.<sup>1a,8</sup> A formal potential of  $E^\circ_M = -0.82$  V vs Fc is thereby measured for the couple of eq 3.<sup>27</sup> At low



temperatures and higher scan rates a second, irreversible wave, attributed to the dimer, grew in at more negative potentials. At  $T = 243$  K, the second wave increased relative to the first until about  $v = 50$  V/s, above which no further relative changes were apparent. In Figure 2 the lower right trace represents this fast scan (frozen equilibrium) limit.

**III. CpCr(CO)<sub>3</sub> Simulations and Dimerization Rate Constants.** Typical background-subtracted and resistance-corrected CV scans of solutions of **2/2**<sub>2</sub> at subambient temperatures are displayed in Figure 2. Figure 3 shows how the raw voltammograms were sequentially treated to obtain the final CV curves of Figure 2. At  $v = 100$  V/s at  $T = 243$  K, the raw CV of a 0.7 mM solution of **2/2**<sub>2</sub> is as seen in Figure 3a. Simple background subtraction yields the dashed line in Figure 3b, and full resistance-corrected background subtraction gives the solid line in Figure 3b. The last line is the

(26) Moulton, R.; Weidman, W.; Vollhardt, K. P. C.; Bard, A. J. *Inorg. Chem.* **1986**, *25*, 1846.

(27) An  $E^\circ$  for **2** in ref 13d was given as  $-0.21$  V vs Ag/AgCl. The formal potential of  $-0.82$  V vs Fc should be considered as the more reliable number; the shift in  $E^\circ$  of  $-0.11$  V we report in going from **2** to **3** is consistent with the literature<sup>13d</sup> shift of  $-0.12$  V. The formal potential of  $-0.82$  V is also consistent with results on the analogous Mo complexes and the potential of **2** in CH<sub>3</sub>CN.<sup>12,13e,f</sup> We thank M. Tilset for pointing this out.

(23) Feldberg, S. W. *J. Electroanal. Chem. Interfacial Electrochem.* **1990**, *290*, 49.

(24) Flanagan, J. B.; Margel, W.; Bard, A. J.; Anson, F. C. *J. Am. Chem. Soc.* **1981**, *100*, 4248.

(25) Evans, D. H.; O'Connell, K. M. In *Electroanalytical Chemistry*; Bard, A. J., Ed.; Marcel Dekker: New York, 1986; Vol. 14, p 113.

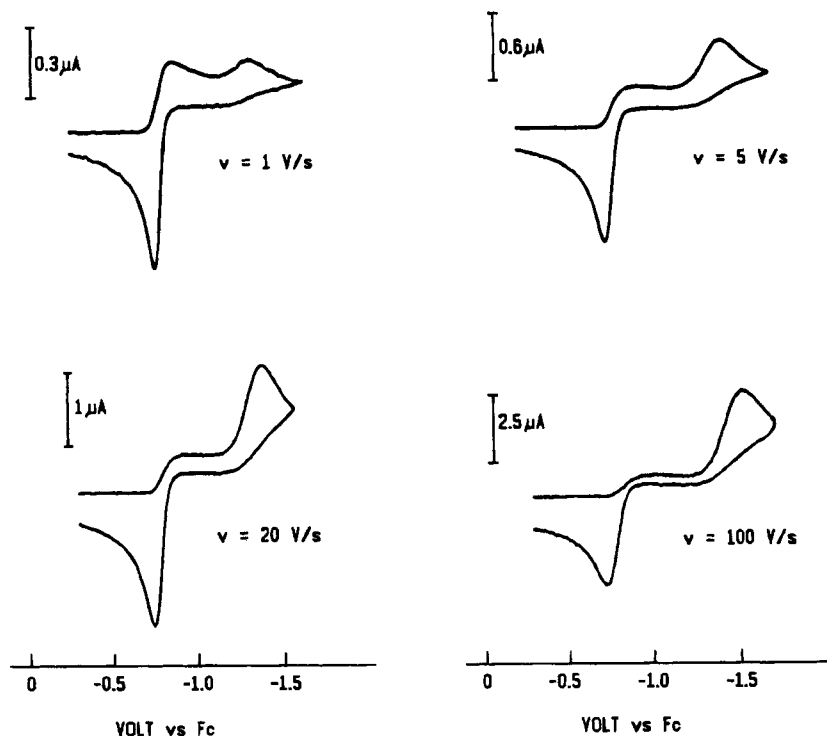


**Figure 2.** Experimental CV curves of a 0.7 mM solution of **2** in  $\text{CH}_2\text{Cl}_2/0.1 \text{ M } [\text{Bu}_4\text{N}][\text{PF}_6]$  at 243 K at a Pt disk (diameter 495  $\mu\text{m}$ ). Scan rates are indicated. Curves have been background subtracted and resistance corrected.

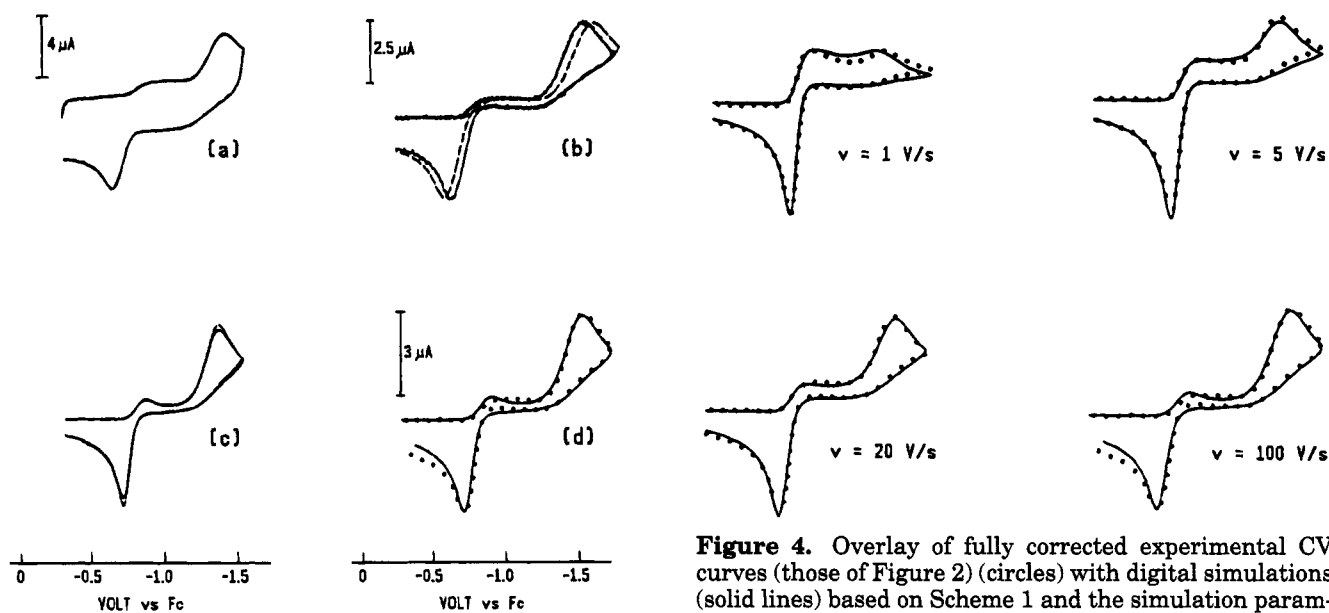


**Figure 3.** Illustration of a full set of correction and the fitting procedure of CV data: (a) raw (i.e., uncorrected) CV of 0.7 mM **2** at 243 K ( $v = 100 \text{ V/s}$ ); (b) same raw CV treated by background subtraction (dashed line) and then by resistance correction (solid line, i.e., fully corrected data); (c) digital simulations with constant scan rate (dashed line) and variable scan rate (solid line); (d) overlay of fully corrected data (circles) with variable scan rate simulation.

“experimental” voltammogram against which theoretical simulations were matched. Figure 3c shows the result of a digital simulation with either constant scan rate (dashed line) or variable scan rate (solid line; see Experimental Section for details). It is seen that the nuances of scan rate variations during the scan, arising from ohmic effects, measurably distort the wave at points following portions of the CV in which the currents

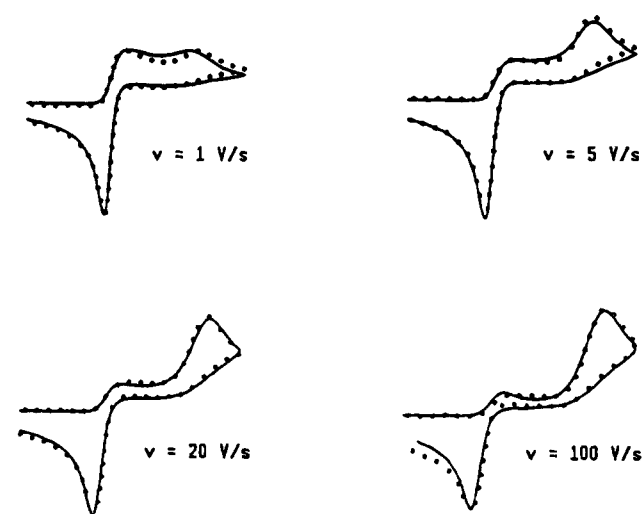


**Figure 4.** Overlay of fully corrected experimental CV curves (those of Figure 2) (circles) with digital simulations (solid lines) based on Scheme 1 and the simulation parameters found in Tables 1 and 2.

are rapidly changing, e.g., near the peak currents and near the switching potential. It is the solid line, therefore, that was used as the digital simulation to match the experimental CV curve. Figure 3d gives the final overlay of theory and experiment for this scan rate.

Adequate matches between theory and experiment were obtained (Figure 4) over a scan rate range of at least 100-fold with a single set of simulation parameters. These parameters are given in Tables 1 and 2. Note that the ET parameters for reduction of the *dimer* are not unique: the  $k_D^\circ$  and  $\alpha_D$  values provide a rationalization of the shape and peak shifts of the second cathodic peak, but other values of  $E_D^\circ$ ,  $k_D^\circ$ , and  $\alpha_D$  would undoubtedly be found to give the same result. The exact parameters chosen, however, for this highly irreversible

**Table 1.** Electrochemical Parameters Associated with the Couples  $\text{CpCr}(\text{CO})_3^{0/-}$ ,  $\text{Cp}^*\text{Cr}(\text{CO})_3^{0/-}$ , and the Corresponding Dimers<sup>a</sup>

compd	$E^\circ_{\text{M}}^b$ (V)	$k^{\circ}_{\text{M}}^c$	$\alpha_{\text{M}}$	$E^\circ_{\text{D}}^b$ (V)	$k^{\circ}_{\text{D}}^c$	$\alpha_{\text{D}}$	temp (K)
$\text{CpCr}(\text{CO})_3^{0/-}$	-0.82	0.06	0.40				243
$[\text{CpCr}(\text{CO})_3]_2^{0/-}$				-1.22 <sup>d</sup>	0.002	0.30	243
$\text{Cp}^*\text{Cr}(\text{CO})_3^{0/-}$	-0.93	0.06	0.40				228
$[\text{Cp}^*\text{Cr}(\text{CO})_3]_2^{0/-}$				-1.33 <sup>d</sup>	0.002	0.30	228

<sup>a</sup> Conditions:  $\text{CH}_2\text{Cl}_2/0.1 \text{ M } [\text{Bu}_4\text{N}][\text{PF}_6]$ ; all parameters from digital simulations. <sup>b</sup> Vs ferrocene/ferrocenium at 243 K. <sup>c</sup> Heterogeneous electron transfer rate (in  $\text{cm}^2/\text{s}$ ) at Pt electrode. <sup>d</sup> Approximate value of rate-limiting one-electron process. Dimer reduction is an overall two-electron process.

**Table 2.** Kinetic Parameters ( $k_{\text{M}}$ ,  $k_{\text{D}}$ ) and Equilibrium Constant  $K_{\text{eq}}$  ( $=k_{\text{M}}/k_{\text{D}} = [\text{M}]^2/[\text{D}]$ ) for Radicals and Their Dimers

monomer	temp	$k_{\text{D}}$ ( $\text{M}^{-1} \text{ s}^{-1}$ )	$k_{\text{M}}$ ( $\text{s}^{-1}$ )	$K_{\text{eq}}$ (M)	comments
$\text{CpCr}(\text{CO})_3$	243 K	$8.4 \times 10^5$	11	$1.3 \times 10^{-5}$	$\text{CH}_2\text{Cl}_2$ , this work
$\text{CpCr}(\text{CO})_3$	RT <sup>d</sup>	$3.0 \times 10^8$	$1.2 \times 10^5$	$4.5 \times 10^{-4}$	THF, ref 10
$\text{Cp}^*\text{Cr}(\text{CO})_3$	228 K	$1.7 \times 10^7$	$3.0 \times 10^3$	$1.8 \times 10^{-4}$	$\text{CH}_2\text{Cl}_2$ , this work
$\text{Cp}^*\text{Cr}(\text{CO})_3$	RT <sup>d</sup>	$7.0 \times 10^6$	$5.6 \times 10^5$	$8.0 \times 10^{-2}$	$\text{CH}_3\text{CN}$ , ref 10

<sup>a</sup> Value determined by IR and optical spectroscopy in ref 8. <sup>b</sup> Value extrapolated from  $K_{\text{eq}}$  determined at 223 and 233 K by IR spectroscopy in ref 1a. <sup>c</sup> Value taken from average of magnetic susceptibility data and IR spectroscopy in ref 1a. <sup>d</sup> Room temperature.

process have virtually no influence on the rate constants  $k_{\text{M}}$  and  $k_{\text{D}}$ , which are the principal objects of our study. The  $E^\circ_{\text{D}}$  value found is expected to be within ca 0.1 V of the true  $E^\circ_{\text{D}}$ .<sup>28</sup>

The value of  $K_{\text{eq}}$  ( $1.25 \times 10^{-5} \text{ M}$ , Table 2) is qualitatively consistent with the findings of McLain, who determined by spectroscopy that a 2 mM solution of  $2/2_2$  in toluene has only dimer present below 238 K.<sup>8</sup> Under the present electrochemical conditions (243 K, 0.7 mF) the mixture is almost 90% dimer. The rate constant found for cracking of the dimer,  $k_{\text{M}} = 11 \text{ s}^{-1}$ , is consistent with the fact that in CV scans dimer to monomer conversion is almost frozen out at  $v = 10 \text{ V/s}$  and is completely frozen at  $v = 100 \text{ V/s}$ .

The dimerization rate constant  $k_{\text{D}} = 8.4 \times 10^5 \text{ M}^{-1} \text{ s}^{-1}$  (Table 2) is lower by a factor of 370 than that measured spectroscopically at room temperature ( $3 \times 10^8 \text{ M}^{-1} \text{ s}^{-1}$ ).<sup>10</sup> It is speculative to compare rate constants obtained at such different temperatures without knowledge of the  $\Delta H^\ddagger$  values, especially when the transition-state structure is in doubt (vide infra). It would appear, however, that any reasonable extrapolation of the electrochemically derived dimerization rate to a higher temperature would still leave the value below that of the photochemically derived value. The presence of supporting electrolyte is not expected to greatly influence the dimerization rate unless a disproportionation mechanism is involved, in which case one would expect the rate to also be strongly influenced by solvent polarity. The fact that the spectroscopically derived rate constant is virtually independent of solvent<sup>10</sup> argues against disproportionation being an important factor. Our electrochemically derived dimerization rate constant seems genuinely lower, therefore, than that previously reported for  $\text{CpCr}(\text{CO})_3$ .

#### IV. Study of $\text{Cp}^*\text{Cr}(\text{CO})_3$ Reduction and Dimerization.

Given the greater steric hindrance to forma-

(28) This number is based on the maximum shift in peak potential away from that of the reversible value for a Nernstian charge transfer system followed by a diffusion-controlled dimerization reaction. See: Saveant, J. M.; Vianello, E. *Electrochim. Acta* **1967**, *12*, 1545. See also the summary treatment in: Bard, A. J.; Faulkner, L. R. *Electrochemical Methods*; Wiley: New York, 1980; p 454.

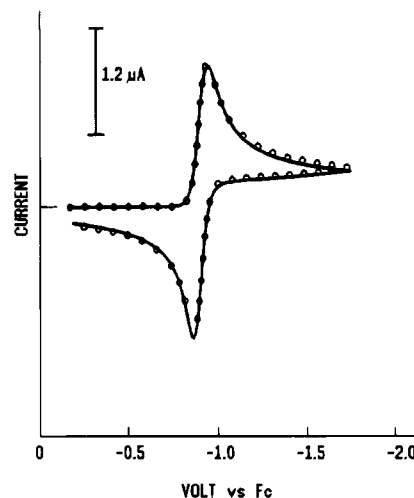
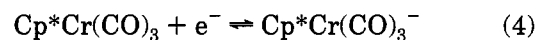


**Figure 5.** Comparison of experimental CV scan (circles) of 0.6 mM **3** in  $\text{CH}_2\text{Cl}_2/0.1 \text{ M } [\text{Bu}_4\text{N}][\text{PF}_6]$  (248 K,  $v = 5 \text{ V/s}$ ) at a Pt disk (495  $\mu\text{m}$  diameter) and digital simulation (solid line) of a Nernstian system with  $E^\circ = -0.93 \text{ V vs Fc}$ .

tion of the dimer when the cyclopentadienyl ligand is permethylated, it is expected that the rate of dissociation of  $[\text{Cp}^*\text{Cr}(\text{CO})_3]_2$  (**3**<sub>2</sub>) will be faster than that of **2**<sub>2</sub>. This is dramatically demonstrated by Figure 5, which is the CV scan of 0.60 mM **3/3**<sub>2</sub> at 248 K with  $v = 5 \text{ V/s}$ . In spite of the fact that the solution contains ca. 40% dimer (relative to the formal concentration) under these conditions, no wave for reduction of the dimer is seen. Conversion of dimer to monomer is complete, therefore, in the time frame of the scan (ca. 100 ms), giving a Nernstian-shaped wave for the reduction of the monomer (eq 4);  $E^\circ_{\text{M}} = -0.93 \text{ V vs Fc}$ .<sup>27</sup> It should be noted



that whereas the  $\text{Cp}^*$  system is in the *slow* scan limit, under identical conditions the  $\text{Cp}$  system was in the *fast* scan limit (frozen equilibrium). The direction of the shift of  $E^\circ$  (-110 mV) from that measured for  $\text{CpCr}(\text{CO})_3$  is as expected from the substitution of  $\text{Cp}$  by  $\text{Cp}^*$ , but the magnitude is only about half of that seen, for example, in ferrocene derivatives.<sup>29</sup>

We did not experience the same quantitative success in digital simulations of experimental fast scan voltammograms as was had with **2**, in part owing to the requirement of even lower temperatures and higher scan rates to outrun the kinetics of the monomer/dimer equilibration. At  $T = 228 \text{ K}$  a sweep rate of ca 200 V/s was required just to view the presence of the dimer wave (Figure 6). Since repeated attempts at background subtraction gave unsatisfactory results,<sup>14</sup> we decided to compare the raw CV curves with digital simulations to estimate the rates  $k_{\text{M}}$  and  $k_{\text{D}}$  for the system **3/3**<sub>2</sub>.

As demonstrated in Figure 6, reasonable agreement was obtained. Experiments at  $v = 200 \text{ V/s}$  (Figure 6, top left) and  $v = 2000 \text{ V/s}$  (top right) are in semiquantitative agreement with the simulated traces (Figure 6, bottom) when using  $k_{\text{M}} = [3.0(\pm 2.1)] \times 10^3 \text{ M}^{-1} \text{ s}^{-1}$ . These simulations used the  $K_{\text{eq}}$  value determined by Hoff et al.<sup>1a</sup> at this temperature ( $1.85 \times 10^{-4} \text{ M}$ ), which

(29) Robbins, J. L.; Edelstein, N.; Spencer, B.; Smart, J. C. *J. Am. Chem. Soc.* **1982**, *104*, 1882.

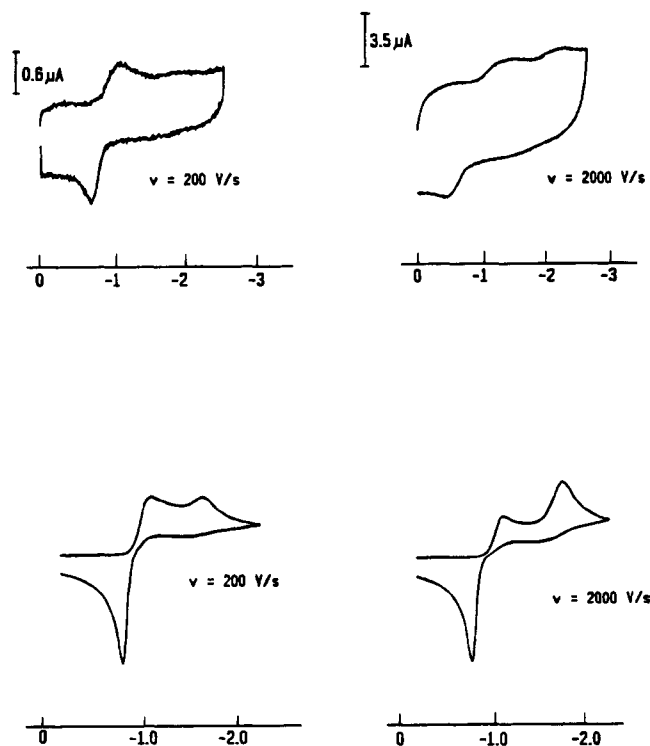


**Figure 6.** Comparison of raw experimental CV traces (top) with theoretical calculations (bottom) for **3**. Experimental conditions: 2.0 mM **3** in  $\text{CH}_2\text{Cl}_2/0.2 \text{ M } [\text{Bu}_4\text{N}][\text{PF}_6]$ ,  $T = 228 \text{ K}$ ,  $125 \mu\text{m}$  diameter Pt disk, scan rates as shown. Theory: digital simulations using parameters given in Tables 1 and 2.

reproduced within expectations the relative cathodic peak heights in the fast scan experimental limit (Figure 6, lower right).

The value of  $k_D$ , the dimerization rate of **3**, can then be calculated from  $k_M$  and  $K_{\text{eq}}$ , yielding  $k_D = 1.7 \times 10^7 \text{ M}^{-1} \text{ s}^{-1}$  at 228 K (Table 2). Remarkably, this value is considerably *higher* than that of the Cp analogue **2** ( $8.4 \times 10^5 \text{ M}^{-1} \text{ s}^{-1}$ ) even at a 15 K colder temperature. Taking into account the temperature difference, the dimerization rate of **3** is 1 or more orders of magnitude larger than that of **2**. This result appears to be at variance with the spectroscopically determined value of  $k_D$  for this system, which (at ambient temperatures) was lower than that of the Cp analogue by a factor of approximately 40.<sup>10</sup>

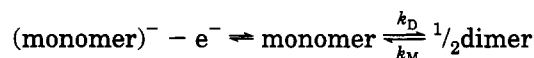
## Discussion

### I. Comments on Electrochemical Strategies.

Two principal electrochemical strategies may be used to determine dimerization rate constants for 17e radicals. In the first (Scheme 2), one starts with the 18e precursor (e.g., the corresponding monoanion  $\text{M}^-$ ) and oxidizes it by one electron. The ratio of the reverse-to-forward currents<sup>30</sup> can be used to measure the dimerization rate constant  $k_D$ , since the reverse current provides a direct measurement of the 17e monomer concentration. As with our alternative approach (vide infra), the M/D equilibrium must favor the dimer for

this method to be successful. In mechanistic terms, this is an EC process with a second-order chemical reaction following electron transfer.

### Scheme 2



Through the use of ultramicroelectrode technology and the availability of very high CV scan rates, the rate constants accessible in this approach rival those of flash photolysis studies. Kochi and co-workers<sup>31</sup> have studied the oxidation of  $[\text{Mn}(\text{CO})_{5-n}\text{L}_n]^-$  ( $n = 0-2$ ;  $\text{L} = \text{PR}_3$ ) and extracted dimerization rate constants of  $\text{Mn}(\text{CO})_{5-n}\text{L}_n$  in excess of  $10^8 \text{ M}^{-1} \text{ s}^{-1}$ , in good agreement with those measured photolytically.<sup>32</sup> This approach works especially well for systems in which the M/D equilibrium strongly favors the dimer. It has also been shown that oxidation of  $[\text{CpMo}(\text{CO})_3]^-$  in this manner results in formation of the Mo-Mo-bonded dimer  $[\text{CpMo}(\text{CO})_3]_2$ , although no dimerization rate constants have been published from these measurements.<sup>12,13b</sup>

A second strategy, employed in the present work, has advantages when detectable amounts of the 17e monomer are present at equilibrium. Under the assumption that the monomer is more easily reduced than the dimer, when the scan reaches the potential of the monomer reduction, some depletion of the reactant (monomer) occurs and additional reactant is furnished by homolysis of the dimer. The increase in cathodic current for  $\text{M} + e^- \rightarrow \text{M}^-$  is proportional to the additional monomer produced during the potential sweep and can be related to the rate constant  $k_M$ . Mechanistically, this is a CE mechanism, with a dimerization reaction preceding electron transfer.

**II. Comparison with Photolytically Derived Rate Constants.** Electrochemistry is an inherently milder method for equilibrium perturbations for these systems than is photolytic excitation. A number of studies have shown that excitation of the dimers  $[\text{CpM}(\text{CO})_3]_2$  may give rise to CO loss from the radical as well as from the dimer, resulting in complex reaction schemes, perhaps best documented for  $\text{M} = \text{Mo}$ .<sup>16</sup> The fact that all species are accounted for in our CV scans assures that such complications are not occurring in the electrochemical experiments but do not, of course, prove that they are occurring in photochemical experiments on the  $\text{M} = \text{Cr}$  system. The lower temperatures used in the electrochemical experiments should also have the effect of minimizing side reactions.

Although the electrochemically derived rate constant for dimerization of  $\text{CpCr}(\text{CO})_3$ ,  $k_D(\mathbf{2})$ , is much lower than that reported by Espenson and co-workers,<sup>10</sup> some of the difference may arise from temperature effects, which are hard to estimate for this system.

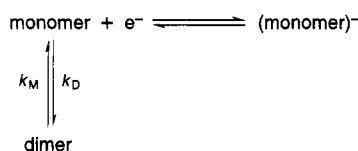
More serious questions are raised, however, concerning the dimerization rate of  $\text{Cp}^*\text{Cr}(\text{CO})_3$  (**3**). The electrochemically derived value of  $k_D = 1.7 \times 10^7 \text{ M}^{-1} \text{ s}^{-1}$  is only marginally larger than the photochemically derived value ( $7 \times 10^6 \text{ M}^{-1} \text{ s}^{-1}$ ), but the latter was obtained at a temperature about 70 K higher than the

(30) Besides cyclic voltammetry, other reversal techniques such as double-potential-step chronoamperometry or -coulometry could also be employed. For leading references to the potential step experiments, see: Murray, R. W. In *Physical Methods of Chemistry*; Rossiter, B. W., Hamilton, J. F., Eds.; Wiley: New York, 1986; Vol. II, Chapter 6.

(31) Kochi, J. K. In *Organometallic Radical Processes*; Troglor, W. C., Ed.; Elsevier: Amsterdam, 1990; pp 205-208.

(32) Walker, H. W.; Herrick, R. S.; Olsen, R. J.; Brown, T. L. *Inorg. Chem.* **1984**, *23*, 3748.

## Scheme 3



former. There does not appear to be a straightforward rationalization of the differences between the two sets of measurements. Both the photolytic and electrochemical results agree, however, that the dimerization of the  $M = \text{Cr}$  complex is much slower than that found for  $M = \text{Mo}^{1b,9a,9b}$  or  $\text{W}^{1b,9c}$  for the radicals  $\text{CpM}(\text{CO})_3$ .

**III. Comparison of Dimerization Rates of Two Cr Monomers.** The most unexpected result to come from the present study is that the dimerization rate of **3**, with its pentamethylcyclopentadienyl group, is *faster* than that of **2**. Certainly, steric bulk *hinders* the formation of dimers from a thermodynamic point of view; therefore it is hard to see why a similar trend would not pertain also to the kinetics of the dimerization. One possible rationalization of the increased dimerization rate of **3** is that the SOMO of the  $\text{Cp}^*$  derivative is more diffuse than that of the  $\text{Cp}$  derivative, allowing more facile interaction between the two radical centers, even though the equilibrium  $M-M$  bond is ultimately longer in **3**. Since the SOMO points away from the  $\text{C}_5\text{R}_5$  ring in these radicals,<sup>6</sup> the steric effects on dimerization rates would thereby be minimized.

Related reasoning arises when one considers the unusually long metal-metal bond in the two dinuclear systems. The  $\text{Cr}-\text{Cr}$  distance in  $[\text{Cp}^*\text{Cr}(\text{CO})_3]_2^{1a}$  (3.311 Å) is only slightly longer than that of  $[\text{CpCr}(\text{CO})_3]_2$  (3.231 Å),<sup>2</sup> both  $M-M$  distances being far longer than expected for a single  $\text{Cr}-\text{Cr}$  bond (ca. 2.8 Å). The weakened  $M-M$  bond accounts, of course, for the ready dissociation of the dimers, and the longer  $\text{Cr}-\text{Cr}$  distance in **3**<sub>2</sub> is consistent with its being more extensively dissociated than **2**<sub>2</sub>.

The thermochemical measurements of Hoff and co-workers show, however, that the greater dissociation of **3**<sub>2</sub> arises from entropic rather than enthalpic (bond strength) considerations.<sup>1a</sup> They point out that the  $\text{Cp}$  complex **2**<sub>2</sub> is already displaced almost 0.5 Å toward dissociation and argue that it is not clear how additional

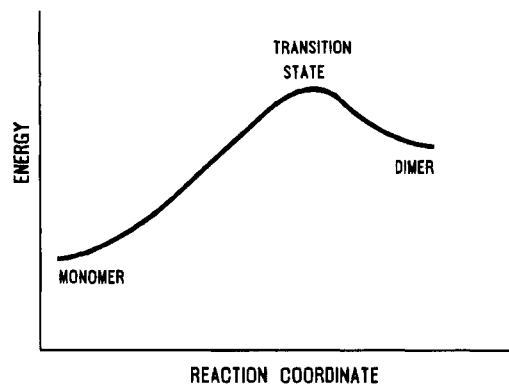


**Figure 7.** Qualitative representation of an energy change in the progress of reaction from monomer to dimer for the  $[(\text{C}_5\text{R}_5)\text{Cr}(\text{CO})_3]_n$  system, implying a transition state structure closer to that of the dimer than to the monomer.

substituents would influence the  $M-M$  bond strength and the potential energy curves for this system.

These thoughts suggest a qualitative reaction coordinate diagram for the monomer/dimer system of Figure 7. Here it is assumed that since only a very small additional lengthening of the  $\text{Cr}-\text{Cr}$  bond is needed to form monomers, the transition state must lie close in structure to that of the dimer.<sup>33</sup> In this situation it is uncertain how the transition-state energy will be affected by the relative influences of steric vs electronic effects. Certainly, more studies are needed of systems with weak metal-metal bonds before working hypotheses concerning the factors controlling their dimerization rates can be confidently formulated.

**Acknowledgment.** This work was generously supported by the National Science Foundation (Grant No. CHE 91-16332). We are grateful to D. H. Evans for helpful advice on the CV simulations, to M. Tilset for permission to quote results in advance of publication,<sup>12</sup> and to J. H. Espenson for valuable comments on details of the photochemical experiments detailed in ref 10.

OM940466O

(33) This is essentially a description of a "late" transition state. See: Salem, L. *Electrons in Chemical Reactions*; Wiley: New York, 1982; pp 47-53.